

# Quantum electronic transport through supported Si<sub>29</sub>H<sub>24</sub> clusters on an ideal Si[111] surface

Samuel E. Baltazar,<sup>1,a)</sup> Mario De Menech,<sup>2,3</sup> Ulf Saalman,<sup>3</sup> Aldo H. Romero,<sup>4</sup> and Martin E. Garcia<sup>2</sup>

<sup>1</sup>Advanced Materials Department, IPICYT, Camino Presa San José 2055, 78216 San Luis Potosí, Mexico

<sup>2</sup>Theoretische Physik, Fachbereich Naturwissenschaften, and Center for Interdisciplinary Nanostructure Science and Technology (CINSA-T), Universität Kassel, Heinrich-Plett-Str. 40, 34132 Kassel, Germany

<sup>3</sup>Max-Planck-Institut für Physik Komplexer Systeme, Nöthnitzer Str. 38, 01187 Dresden, Germany

<sup>4</sup>CINVESTAV Querétaro, Libramiento Norponiente No. 2000, 76230 Querétaro, Mexico

(Received 15 June 2007; accepted 29 November 2007; published online 31 January 2008)

We report calculations of the current-voltage ( $I$ - $V$ ) characteristics and the differential conductance of a Si<sub>29</sub>H<sub>24</sub> cluster supported on an ideal Si[111] surface. Firstly, the distance between cluster and surface was optimized using *ab initio* calculations. Then, the electron transport was calculated by means of an extended Hückel model combined with a self-consistent calculation of the nonequilibrium Green's functions. We find that the bond formation between cluster and surface leads to changes in the density of states of the cluster. The peak associated with this bond is located inside the energy gap of Si[111] diminishing its effect on the  $I$ - $V$  characteristics, which exhibits a diodelike behavior. Finally, we determine the conductance spectra and characterize the charge distribution of the states which mainly contribute to transport at different bias voltages. © 2008 American Institute of Physics. [DOI: 10.1063/1.2838172]

## I. INTRODUCTION

Transport properties through molecules have been extensively studied with the goal of manufacturing nanoscale electronic devices. At this level, the interaction between a supported molecule on top of any surface and a metallic electrode or a scanning tunneling microscope (STM) tip has an important influence on the transport properties. In the case of a molecule placed between metallic contacts, which have almost constant densities of states (DOS), the  $I$ - $V$  characteristics is determined by the wave functions of the molecule for bias voltages covering the energy range of allowed molecular states. On the other hand, if we use contacts with a more complex DOS, like a semiconductor, the electronic transport and the properties of the device will change. In recent years, different investigations were conducted in order to understand the effect of molecules supported by semiconducting surfaces. In this setup, a STM probe is used as a second electrode and the applied potential can control the electronic transport. The use of surfaces with band gaps and active electronic states could provide the ingredients for phenomena that are not observed with metallic surfaces.

Silicon clusters have been subjects of many experimental and theoretical studies in the last years. For example, Belomoin *et al.*<sup>1</sup> have reported a dependence of the optical response of silicon clusters on different terminations (C, N, H) and on the cluster size (1–3 nm). They discussed the possible application of these clusters for biological imaging. Another reason for studying these particles is that they are easy to produce (usually formed in solution), with a stable

and reproducible structure and most of them are optically active. Usually, clusters are different from the bulklike structure, mainly due to surface effects since the surface-to-volume ratio becomes important.

In studies of transport properties of devices containing metallic nanocrystals and organic molecules, a diodelike behavior has been observed.<sup>2,3</sup> These results encouraged applied physicists to consider the development of nanoelectronic devices by using silicon clusters as active structures. In this direction, deposition of small silicon clusters on silicon surfaces has been reported by Watanabe *et al.*<sup>4</sup> Scanning tunneling spectroscopy (STS) measurements were performed on these samples and they were able to show resonant tunneling on those devices due to electronic states of the cluster.<sup>5</sup>

STS is the optimal tool to investigate the interaction of clusters on surfaces. In this paper, we propose that similar properties in the electronic transport can be attributed to molecular levels and the electronic states obtained in the bonding of the molecule with the surface. The electronic properties are described in the framework of an extended Hückel model (EHT). The methodology has been tested comparing the electronic properties with *ab initio* calculations. Using an effective single-particle Hamiltonian, we performed a systematic study for different cluster-surface configurations, surface doping, and bias voltages. The electronic density is studied as a function of the applied bias specifically for the states located near the Fermi level of the surface.

## II. THEORY

In this section, we briefly summarize the theoretical approach we used to describe the electronic transport through Si<sub>29</sub>H<sub>24</sub> clusters supported on a Si surface and probed by a

<sup>a)</sup>Electronic mail: sbaltaza@ipicyt.edu.mx. Also at Theoretische Physik, Fachbereich Naturwissenschaften, Universität Kassel, Heinrich-Plett-Str.40, 34132 Kassel, Germany.

flat electrode. In order to describe the entire system (substrate-cluster-electrode), we have considered an ideal surface structure, a cluster, and a STM probe (see Fig. 1). An *ab initio* calculation is performed to optimize the cluster-surface distance (see below). Then, all components remain fixed during the voltage application and transport measurements. Electronic properties at equilibrium and transport properties at nonequilibrium conditions were calculated using a Green's function approach.<sup>6,7</sup> In particular, we use the method presented by De Menech *et al.*<sup>8,9</sup> For infinite separation between the electrode, the cluster, and the surface, the system is described by the molecular Hamiltonian  $H_{\text{mol}}$  and the contact Hamiltonian  $H_C$  (surface and electrode). At equilibrium, the coupled system (contacts  $C$ +cluster) is described by the Hamiltonian  $H$  which is comprised of  $H_{\text{mol}}$ ,  $H_C$ , and terms accounting for the couplings. Green's function  $G$  of the total system follows from the composite Schrödinger equation

$$[(E + i\eta)S - H]G(E) = 1, \quad \eta \rightarrow 0^+, \quad (1)$$

where  $S$  is the overlap matrix of the wave functions. In the Green's function approach, it is possible to write the spectral function (density of states per unit energy) as

$$A(E) = -\frac{2}{\pi} \text{Im}[G(E)], \quad (2)$$

for the spin unpolarized case (simple generalization can be done for the polarized case). Then, it is possible to obtain the local density of states as

$$\rho(r, E) = \sum_{\mu\nu} A_{\mu\nu}(E) \psi_\mu \psi_\nu, \quad (3)$$

where  $\psi$  are the molecular wave functions and the total electronic density

$$n(r) = \int_{-\infty}^{E_F} dE \rho(r, E), \quad (4)$$

which considers integration until the Fermi energy level  $E_F$ . Now, if we want to study the consequences on a specific part of the system, for instance, the cluster, the Green's function approach allows to represent it with contributions from the other parts, for instance, from the contacts. This approach has been described by Williams *et al.*<sup>6</sup> to study crystals with defects as perturbations showing that the problem can be described by a Dyson equation to get Green's function of the perturbed system. In our case, the Dyson equation leads to the perturbed Green's function of the cluster, considering the surface effects as

$$G(E) = G^0(E) + G^0(E)\Sigma G(E), \quad (5)$$

where  $G^0$  and  $G$  are Green's functions associated with the isolated cluster (unperturbed case) and the supported cluster (perturbed), respectively, and  $\Sigma$  is the self-energy matrix,

$$\Sigma = \tau G_s^0(E) \tau^\dagger, \quad (6)$$

that takes into account the effect of the surface such as broadening and shifting of molecular energy levels (the size of  $G$ ,  $G^0$ , and  $\Sigma$  are defined by the number of the molecular

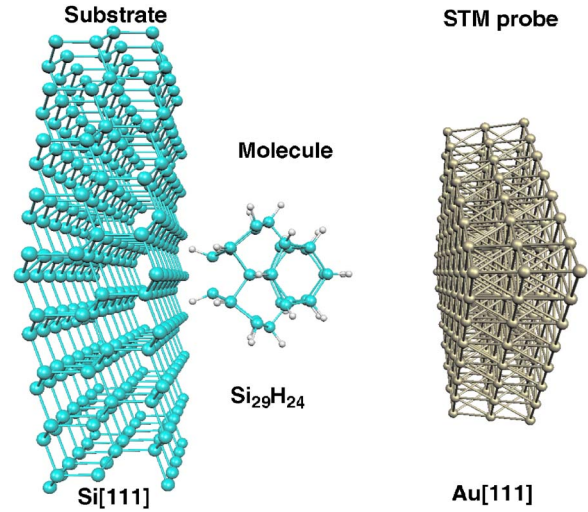


FIG. 1. (Color online) Atomic configuration of the silicon cluster interacting, at a given optimal distance, with a semiconducting surface Si[111] and a metallic electrode Au[111] used as a STM probe.

orbitals only). The term  $G_s^0(E)$  corresponds to Green's function of the isolated surface and  $\tau$  is the coupling matrix between the cluster and the surface. One is in the nonequilibrium regime when another electrode is added to the system and an external voltage is applied between the surface and the electrode. In this case, the representation for the supported cluster is changed using the correlation function  $G^< = G\Sigma^<G^<$  to determine the charge density at a specific bias  $V$ . The term  $\Sigma^< = i[f(E - \mu_s)\Gamma^s + f(E - \mu_e)\Gamma^e]$  is the lesser self-energy that depends on the chemical potential  $\mu$  and the broadening matrix  $\Gamma$  of the surface and the metallic electrode. The probability at which an electron goes from one contact to another through the cluster is given by the transmittance  $T(E, V)$ . If we want to take into account only coherent transport (no scattering), it is possible to show that  $T(E, V)$  can be evaluated using the relation

$$T \equiv \text{Tr}[\Gamma^s G^e G^\dagger]. \quad (7)$$

Finally, we can calculate the current through a system like the one we are interested in, cf. Fig. 1. The cluster (with discrete energy levels) is located between a semiconductor surface (with gaps in the DOS) and an electrode (with a uniform distribution of states). In this case, the current can be written as

$$I = \frac{2e}{h} \int_{-\infty}^{\infty} dE T(E) [f_1 - f_2]. \quad (8)$$

The transmittance  $T(E)$  is integrated in the energy interval associated with each applied bias voltage and  $f_i = f(E - \mu_i)$  associated with each contact  $i$ . For both cases (surface and electrode), local equilibrium is assumed and the low temperature approximation is used, so the Fermi distribution allows to integrate  $T(E)$  only between  $\mu_1$  and  $\mu_2$ .

After the calculation of the transmittance is performed, we followed the treatment given by Tian *et al.*<sup>10</sup> to obtain the conductance and the differential conductance. At low temperature regime, the conductance will be proportional to the transmittance (calculated at zero voltage and it can be used to

compare the evolution of the states when an external bias is applied), where the differential conductance will be written as

$$\frac{dI}{dV} \approx G_0 T(E_f + eV), \quad (9)$$

where  $G_0 = 2e^2/h$  is the conductance quantum. Here, it is assumed that the electrostatic potential modifies mostly the chemical potential of the metallic electrode. To describe the molecular electronic properties, we use the EHT approach, where the Hamiltonian is parametrized through the matrix elements  $H_{\alpha i, \beta j}$  between two atomic orbitals  $\alpha$  and  $\beta$  of atoms  $i$  and  $j$ , respectively, and assumed to be proportional to the overlap  $O_{\alpha i, \beta j}$  and such that  $H_{\alpha i, \beta j} = K_{\alpha i, \beta j} O_{\alpha i, \beta j}$ . According to Cerda and Soria,<sup>11</sup> the parameter  $K_{\alpha i, \beta j}$  can be defined from the on-site energies using the form  $K_{\alpha i, \beta j} = K_{\text{EHT}} \cdot (E_{\alpha i} + E_{\beta j})/2$ , where  $K_{\text{EHT}}$  is a fitting parameter usually obtained for solids and calculated from first principles.

In order to evaluate the accuracy of this model, we have compared the description obtained with the EHT model, with a calculation based on the code CPMD in a plane wave pseudopotential implementation of density functional theory<sup>12</sup> following a local spin density approximation (LSDA) and using the correlation functional Vosko, Wilk, and Nusair (VWN) combined with the Slater exchange and an expanded basis set 6-311G.<sup>13,14</sup> Furthermore, this theory has been used to calculate the atomic structure by minimizing the energy of the isolated molecule and the supported molecule in contact with the surface.

### III. RESULTS

In order to characterize the coupled system (substrate-molecule), we start by considering the electronic properties of the different components disconnected from each other. After this, the silicon cluster has been located on a silicon semiconductor surface grown along the [111] direction and without reconstruction. Experimentally the surface can exhibit a  $2 \times 1$ ,  $7 \times 7$  reconstruction according to the applied temperature,<sup>4,5</sup> but it is also possible to obtain a Si[111]- $1 \times 1$  structure.<sup>15</sup> The understanding of the transport without reconstruction could also help to disentangle different mechanisms in the case of reconstruction. In this particular case, there are dangling bonds on the unreconstructed surface which are associated with dispersionless energy levels found in the band structure of Si[111]. The band structure has been obtained using 24 layers (depth of 7 nm) and it is found that the electronic and structural properties are in good agreement with theoretical results obtained by Ivanov *et al.*<sup>16</sup>

For the molecule, a *H*-passivated Si<sub>29</sub>H<sub>24</sub> silicon cluster has been selected where the atomic configuration of the cluster in contact with the silicon surface has been geometrically optimized following a LSDA approach. The optimal distance between the silicon cluster and the surface was found to be 2.2 Å (distance between silicon atoms on the surface and hydrogen atoms of the silicon cluster). The silicon surface used to study electronic transport properties is the ideal unreconstructed Si[111] moving the cluster until the calculated optimal distance and fixing the atomic configuration of the

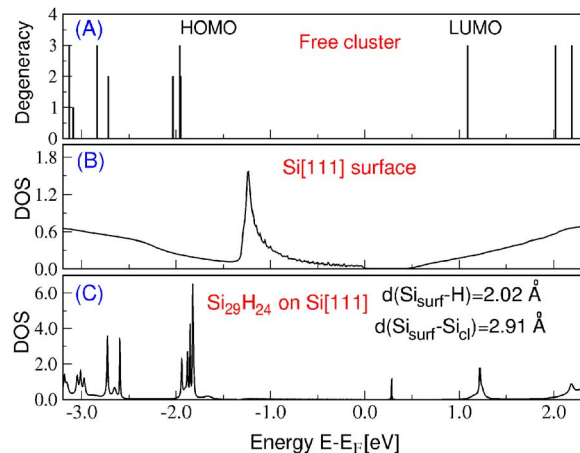


FIG. 2. (Color online) Electronic structure of the system. Graph (A) shows the energy levels for the isolated Si<sub>29</sub>H<sub>24</sub> cluster, (B) shows the DOS of isolated Si[111] surface without reconstruction, and (C) corresponds to the DOS of Si<sub>29</sub>H<sub>24</sub> cluster in contact with the ideal Si[111] surface. Energy values are shifted with respect to the Fermi level ( $-4.36$  eV).

system (cluster and surface). The electronic structure (energy levels in the cluster) is calculated using the EHT approach, where the parameter  $K_{\text{EHT}}$  was fixed at 1.75 and 2.1 for H and Si, respectively.<sup>11</sup> The distribution of calculated molecular energy levels, close to the Fermi level, is in good agreement with the results obtained with a LSDA approach. In particular, the difference between the highest occupied molecular orbital (HOMO) and the lowest unoccupied molecular orbital (LUMO) is 3.04 eV (3.01 eV in the case of LSDA), which is also in good agreement with other studies previously reported and based on first-principles calculations.<sup>1,17</sup>

Figure 2 shows the electronic configurations of the isolated components and the coupled case that has been calculated following the EHT approach. Figure 2(a) corresponds to the discrete energy levels associated with the free cluster Si<sub>29</sub>H<sub>24</sub>. Figure 2(b) corresponds to the DOS of a Si[111] surface where an energy gap of 0.45 eV is observed. In this case, the valence band maximum is located at 4.36 eV and the conduction band minimum is found to be at 3.9 eV. Besides this, the contributions of dangling bonds are present mainly at 1.2 eV below the Fermi level. This description is in good agreement with the results reported by Pandey and Philips<sup>18</sup> and Schlüter *et al.*,<sup>19</sup> obtained using a semiempirical tight-binding method and a self-consistent pseudopotential, respectively. The presence of the dangling bonds is observed in these cases with a general shift of the states compared with our results. After the cluster is absorbed on the surface, a total shift and broadening of molecular levels are found in the e-DOS, as observed in Fig. 2(a). A peak not seen in the free cluster is also found around 0.3 eV above the Fermi level. A similar behavior in the DOS has been observed for different positions of the cluster on the surface keeping the cluster-surface distance fixed.

For the calculation of transmittance, current, and conductance, a second electrode is added as a STM probe represented by a metallic surface (depicted in Fig. 1). This electrode is a planar and ideal Au[111] surface, which happens to be numerically convenient to obtain Green's functions of the

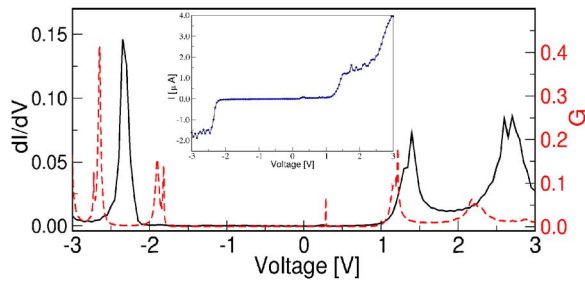


FIG. 3. (Color online) Differential conductance  $dI/dV$  (solid line) and conductance (dashed line) as a function of the applied bias. The inset shows the current for the Si[111]-Si<sub>29</sub>H<sub>24</sub>-Au[111] system as a function of voltage. The optimal cluster-surface distance is 2.2 Å as obtained from a LSDA calculation.

surface based on a periodic cell. Both electrode and surface are initially at local equilibrium with chemical potentials  $\mu_e = -5.26$  eV and  $\mu_s = -4.3$  eV, respectively.<sup>20</sup> In order to consider the total system at equilibrium, we have changed the chemical potential of the metallic electrode forcing it to be at equilibrium with the surface. Then, an external voltage bias  $V$  is applied, whereby  $\mu_e$  is changed and the cluster is embedded in an electric field created by the contacts. In this situation, the transmittance  $T(E, V)$  is calculated and the current at the applied voltage can be obtained by integrating the transmittance function in the specific energy interval associated with each bias  $V$ .

We have also considered doped surfaces, prepared to modify the availability of electrons in the surface. This effect allows to change the number of states close to the Fermi level that are important in transport processes. A simple approach to characterize this effect considers the variation of the chemical potential leading to three regimes: undoped,  $p$ -doped, and  $n$ -doped cases. Another factor is the electrode (tip)-cluster distance  $d$  where the electronic transport properties have been evaluated at  $d=4, 5,$  and  $6$  Å. In this case, the current shows only a change in the intensity in agreement with the exponential decay of current as a function of the distance.

Figure 3 presents the differential conductance  $dI/dV$ , conductance  $G$ , and in the inset the  $I$ - $V$  characteristic for Si<sub>29</sub>H<sub>24</sub> cluster on the surface considering 2.2 Å as the optimal cluster-surface distance. The  $dI/dV$  curve shows the peak distribution as a function of applied voltage. It is important to notice that the peak initially located around 0.3 eV (see  $G$  in Fig. 3) is reported in the conductance but its contribution in the  $dI/dV$  and the  $I$ - $V$  characteristic is barely noticed compared to the next peak located around 1.2 eV above Fermi level and that increased the current at voltages bigger than 1.3 V.

Figure 4 shows the evolution of the states in the DOS when an external bias is applied. In this case, we can see that the small peak at 0.3 eV (charge density of the peak is depicted in the DOS in Fig. 4), obtained from the cluster-surface interaction, does not shift its position, compared to the other states. This behavior can also be observed in Fig. 3 where the differential conductance  $dI/dV$  shows the peak at the same position as the conductance  $G$  (evaluated at equilibrium).

After this, we examine the effect of applying a negative

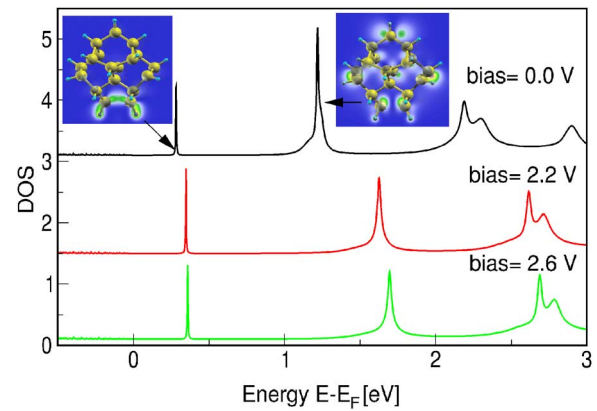


FIG. 4. (Color online) DOS of molecular levels as a function of the applied positive bias. Additionally, charge distributions of the peak located at 0.3 eV (above the Fermi level) and the LUMO level (at 1.2 eV above the Fermi level) are depicted as insets.

bias to see the evolution of the states when the potential profile is given in the opposite direction. In this case, we have considered the highest occupied state (located around  $-1.8$  eV below  $E_F$ ) and showed the voltage effect on the DOS of Si<sub>29</sub>H<sub>24</sub> (see Fig. 5). The charge distribution corresponding to the highest occupied state (A) is depicted in Fig. 5 within the evolution of this state when a bias of  $-3.0$  V is applied (B). As soon as the voltage becomes more negative, peaks are shifted to the left with respect to the surface Fermi level, and the labeled peak in the DOS of the cluster is split into separated states [(B) in Fig. 5].

This evolution is confirmed when we observe the charge distribution associated with this peak (upper figures in Fig. 5). A polarization of the electronic charge in Si<sub>29</sub>H<sub>24</sub> cluster, along the direction perpendicular to the surface, is observed. The initial charge distribution [(A) in Fig. 5], at 0.0 V, shows a nonsymmetrical distribution, whereas when the applied bias is  $-3.0$  V, a symmetrical distribution is obtained.

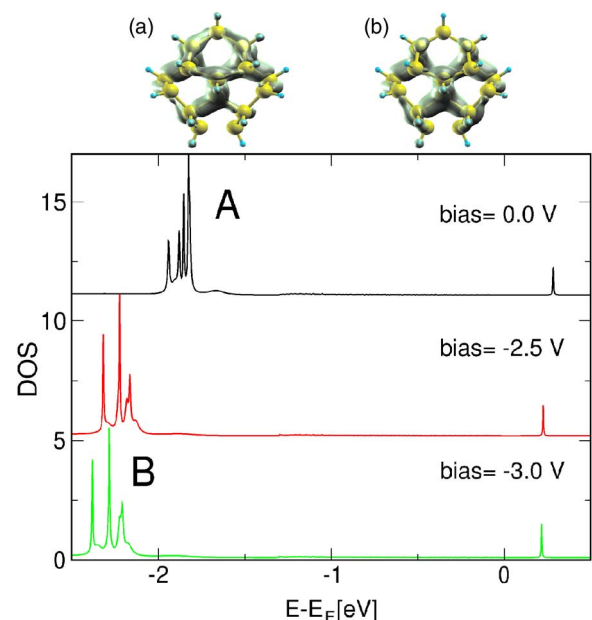


FIG. 5. (Color online) Up figure shows the charge density distribution of Si<sub>29</sub>H<sub>24</sub> associated with a specific peak (HOMO level for the free cluster case) in DOS at 0.0 (A) and  $-3.0$  V (B). The figure below shows the calculated DOS at different applied negative voltages.

We have also considered doped surfaces following a simple approximation based on an artificial shift of the Fermi level in order to simulate the inclusion of dopant atoms, such as P or S, on the surface. Defining the initial chemical potential ( $\mu_s = -4.3$  eV), an *n*-type surface was defined for  $\mu_s = -3.8$  eV, whereas for the *p*-doped case, the chemical potential was fixed at  $\mu_s = -4.8$  eV. For both cases, an energy shift of the DOS is obtained with respect to the initial condition and the *I-V* characteristics shows a similar displacement. Also, if we consider an *n*-type surface ( $\mu_s = -3.8$  eV), the found peak is not inside the energy interval integrated to calculate the current at positive bias but it can be found at the negative voltage regime. The influence of the found peak is still neglected in these cases because it is still localized in the energy gap of the surface (from 0.0 to 0.45 eV). The position of the peak as a function of the doped surface is 0.22 eV for the *p*-type surface, 0.28 eV for the undoped case, and 0.35 eV for the *n*-type surface. Also, the shift of this peak is smaller compared to the other peaks (see DOS in Fig. 4) because this state is associated with the cluster-surface interaction.

#### IV. DISCUSSION AND CONCLUSIONS

Here, we have reported a set of electronic transport calculations for the semiconductor-cluster-metal system. In order to understand the transport mechanism, we consider three cases: (i) Equilibrium case ( $V=0$ ) where  $\mu_1 = \mu_2$ , there is no current flowing from one electrode to another. (ii) For negative bias, the relation  $\mu_2 - \mu_1 = -qV$  shows that there is a flow of electrons from the silicon surface to the STM probe through the molecular energy levels. Notice that the molecular levels are shifted to the left with respect to the surface chemical potential  $\mu_1$  because of the potential created between the electrodes. (iii) For a positive bias, we can see that molecular levels are shifted to the right with respect to the surface chemical potential so we can consider electronic transport due to the presence of unoccupied molecular orbitals and available states in the surface.

At equilibrium, depicted in Fig. 2, the cluster-surface interaction has established a peak in DOS, which can be observed with the charge distribution depicted in Fig. 4. The net charge of the cluster shows that the cluster has transferred electronic charge to the surface due to the interaction and this distribution is modulated by the applied bias under nonequilibrium conditions. The influence of this peak is also diminished in Fig. 3, where the conductance *G* shows the peak around 0.3 eV; in contrast, the *dI/dV* and *I-V* curves show the same peak with almost no perturbation compared to the contribution of the next peak starting at 1.3 eV. This can be explained if we consider that the found peak (at 0.3 eV) is located inside the region associated with the band gap of Si[111]. Also, the cluster-surface interaction is barely affected by the voltage in the range we have applied it, showing that this is a localized state (charge density depicted in Fig. 4) compared to the rest of the molecular states. In the case of negative bias, we can see that the effect of the elec-

trical field promotes a splitting of peak A in Fig. 5. The charge density for this peak (going from A to B) in Fig. 5 have also been redistributed when the bias is increased, leading to a symmetrical distribution (at  $-3.0$  V).

In summary, the extended Hückel model, used to describe the electronic properties in the system, is in good agreement when compared with tight-binding and *ab initio* calculations. For Si<sub>29</sub>H<sub>24</sub> on Si[111], a peak created by the cluster-surface interaction was found in the energy gap of the silicon surface. This gap diminishes the effect of the peak in the *I-V* characteristic as well as in the *dI/dV* case. The created state has a charge distribution close to the surface and its position is unaffected by the external applied bias. On the ranges we study, our results show that the position of molecular levels, with respect to the surface, is important in order to understand molecular electronic transport. A nonmetallic surface has interesting properties with respect to metallic ones, allowing to control transport with the appropriate conditions. In our case, we have a nonconducting behavior of the system at low voltage (positive and negative cases). These results strengthen the idea of using silicon clusters as possible components in large voltage valves or diodes in electronic devices.

#### ACKNOWLEDGMENTS

M.E.G. acknowledges the kind hospitality at the IPICyT. A.H.R. acknowledges support from Conacyt J-59853-F. S.E.B. acknowledges the scholarship given by IPICyT and the University of Kassel and also acknowledges CNS for computational resources.

- <sup>1</sup>G. Belomoin, J. Therrien, A. Smith, S. Rao, R. Twisten, S. Chaieb, N. H. Nayfeh, L. W., and L. Mitas, *Appl. Phys. Lett.* **80**, 841 (2002).
- <sup>2</sup>M. A. Reed, C. Zhou, C. J. Muller, T. P. Burgin, and J. M. Tour, *Science* **278**, 252 (1997).
- <sup>3</sup>D. L. Klein, P. L. McEuen, J. E. B. Katari, R. Roth, and A. P. Alivisatos, *Appl. Phys. Lett.* **68**, 2574 (1996).
- <sup>4</sup>M. O. Watanabe, T. Miyazaki, and T. Kanayama, *Phys. Rev. Lett.* **81**, 5362 (1998).
- <sup>5</sup>L. Bolotov, N. Uchida, and T. Kanayama, *Eur. Phys. J. D* **16**, 271 (2001).
- <sup>6</sup>A. R. Williams, P. J. Feibelman, and N. D. Lang, *Phys. Rev. B* **26**, 5433 (1982).
- <sup>7</sup>H. Haug and A. P. Jauho, *Quantum Kinetics in Transport and Optics of Semiconductors* (Springer-Verlag, Berlin, 1996).
- <sup>8</sup>M. De Menech, U. Saalman, and M. E. Garcia, *Appl. Phys. A: Mater. Sci. Process.* **82**, 113 (2006).
- <sup>9</sup>M. De Menech, U. Saalman, and M. E. Garcia, *Phys. Rev. B* **73**, 155407 (2006).
- <sup>10</sup>W. Tian, S. Datta, S. Hong, R. Reifengerger, J. I. Henderson, and C. P. Kubiak, *J. Chem. Phys.* **109**, 2874 (1998).
- <sup>11</sup>J. Cerda and F. Soria, *Phys. Rev. B* **61**, 7965 (2000).
- <sup>12</sup>Computer code CPMD Version 3.9.2, © IBM Corp. 1990–2001 and © MPI für Festkörperforschung Stuttgart 1997–2001.
- <sup>13</sup>S. H. Vosko, L. Wilk, and M. Nusair, *Can. J. Phys.* **58**, 1200 (1980).
- <sup>14</sup>P. Hohenberg and W. Kohn, *Phys. Rev.* **136**, B864 (1964).
- <sup>15</sup>A. Khan, *Surf. Sci. Rep.* **3**, 193 (1983).
- <sup>16</sup>I. Ivanov, A. Mazur, and J. Pollman, *Surf. Sci.* **92**, 365 (1980).
- <sup>17</sup>G. Allan, C. Delerue, and M. Lannoo, *Phys. Rev. Lett.* **76**, 2961 (1996).
- <sup>18</sup>K. C. Pandey and J. C. Phillips, *Phys. Rev. B* **13**, 750 (1976).
- <sup>19</sup>M. Schlüter, J. R. Chelikowsky, S. G. Louie, and M. L. Cohen, *Phys. Rev. B* **12**, 4200 (1975).
- <sup>20</sup>F. G. Allen and G. W. Gobeli, *Phys. Rev.* **127**, 150 (1962).